JOURNAL OF CATALYSIS **121**, 202–218 (1990)

Ethylene Oxidation on Silver Powder: A Tap Reactor Study

JOHN T. GLEAVES,* ALLEN G. SAULT,† ROBERT J. MADIX‡,[1] AND JERRY R. EBNER§

**Department of Chemical Engineering, Washington University, One Brookings Drive, St. Louis, Missouri 63130; †Sandia National Laboratories, Division 6212, Albuquerque, New Mexico 87185; ‡Department of Chemical Engineering, Stanford University, Stanford, California 94305-5025; and §Monsanto Company, 800 North Lindbergh Boulevard, St. Louis, Missouri 63167*

Received January 31, 1989; revised August 29, 1989

The oxidation of ethylene over silver powder catalysts was studied between 475 and 575 K at pressures of circa 10 Torr under transient conditions that allowed reactions of atomic and molecular oxygen to be distinguished. Dioxygen and d_4-ethylene were pulsed separately over silver powder in a microreactor with pulse durations of 200 μs, and the products were detected by a multiplexed mass spectrometer. This method, denoted as temporal analysis of products, allows either simultaneous pulsing of the reactants or pulse delays ranging from a few milliseconds to minutes. In these experiments both ethylene oxide and carbon dioxide were detected as products. Ethylene oxide formed instantaneously on the time scale of the reactant pulse, but carbon dioxide formed with a much slower time constant, characteristic of the decomposition of surface carbonate, indicating the importance of secondary interactions of CO_2 with surface oxygen in the kinetics of CO_2 formation. Pulse-probe experiments, in which the catalyst was first loaded with adsorbed atomic oxygen and then reacted with anaerobic ethylene pulses or ethylene–oxygen mixtures, showed that the adsorbed species giving rise to ethylene oxide is atomic, not molecular, oxygen.

INTRODUCTION

Commercial production of ethylene oxide is accomplished by the partial oxidation of ethylene over supported silver catalysts. Because of the industrial importance of ethylene oxidation, a great deal of research effort has been directed toward understanding the mechanism of the reaction, and several reviews of the ethylene oxidation literature have been published (*1–4, 25*). Current research is focused on understanding the uniqueness of silver as a selective oxidation catalyst and on discerning the roles of different forms of adsorbed oxygen in the mechanisms of the total and partial oxidation.

Evidence has been advanced in support of several different mechanisms. One mechanism attributes total combustion to reaction with atomic oxygen ($O_{(a)}$) and epoxidation to reaction with molecular oxygen ($O_{2(a)}$) (*1–7*). A second mechanism attributes both combustion and epoxidation to $O_{(a)}$ (*1, 2, 8–12, 18*). Campbell and coworkers originally interpreted their results in terms of the involvement of $O_{2(a)}$ in both epoxidation and total combustion (*13–16*). They have recently offered an alternate interpretation of this data, however, involving a "special" state of atomic oxygen as the active species for ethylene oxidation (*17*). In the work reported in this paper, ethylene oxidation experiments performed using a new transient technique called temporal analysis of products (TAP) (*19*) are reported. The TAP apparatus is basically a pulsed microreactor which allows contact times between the reactant gases and the catalyst on the order of a few milliseconds and provides for variable time delays between pulses of reactants. The short time scale of the pulses and the delay between pulses of oxygen and ethylene afford unique measurements of the lifetime of the reactive intermediate and allow the form of

---

[1] To whom correspondence should be addressed.

0021-9517/90 $3.00

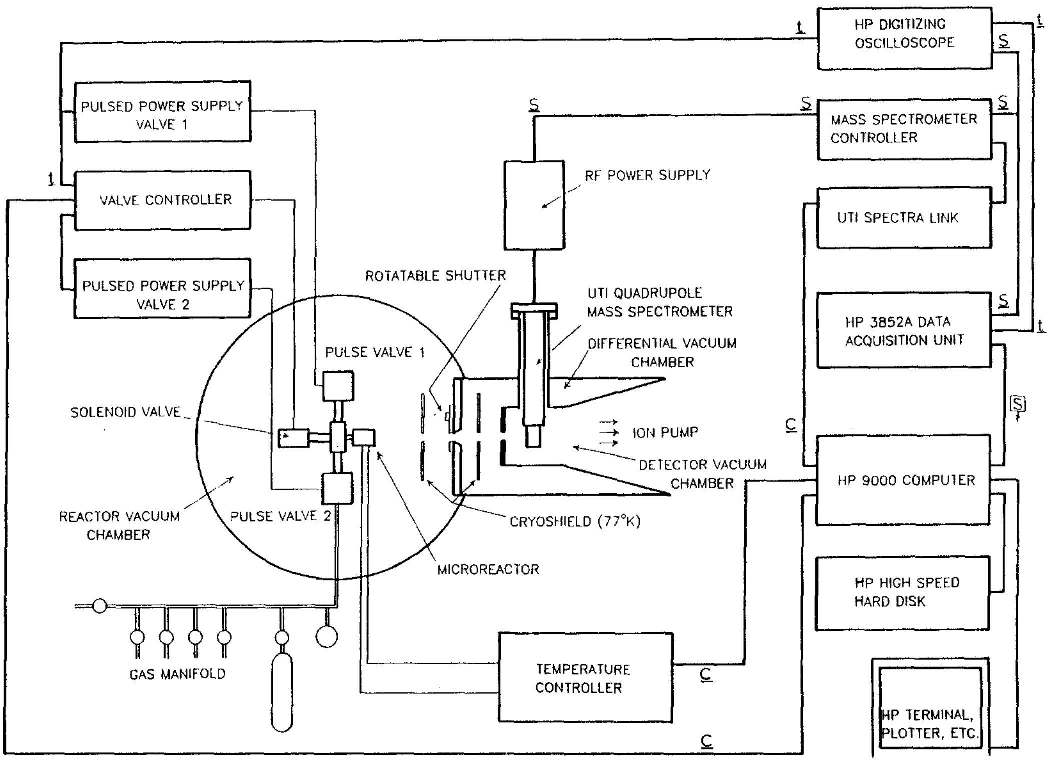

FIG. 1. Schematic diagram of the TAP reactor system.

the adsorbed oxygen which participates in the reaction to be determined. Our results lend further support to the participation of $O_{(a)}$ in both the epoxidation and total combustion reactions of ethylene.

EXPERIMENTAL

The TAP apparatus and data analysis technique are described in detail elsewhere (*19*). Briefly, the apparatus, shown schematically in Fig. 1, consists of a catalytic microreactor, a gas delivery system for introduction of either high-speed gas pulses or a continuous flow of gas, a high-throughput, high-vacuum system, and a computer-controlled, quadrupole mass spectrometer-based detector system. The microreactor is a stainless-steel tube 12.5 mm long and 6.4 mm in diameter. Its temperature can be varied between -100 and 600°C. Catalyst particles are held in place by stainless-steel screens and the temperature in the bed is measured at two points with thermocouples.

The two high-speed pulse valves can deliver up to 50 pulses per second. These pulses have a FWHM of $\sim$200 μs, and the pulse intensities can be varied between 10^{13} and 10^{20} molecules per pulse. In this work, ethylene and oxygen were pulsed through separate valves and, unless otherwise noted, the pulse size was 10^{17} molecules for both reactants. From the pulse size, the reactor volume, and the amount of silver powder in the reactor, a crude estimate of the pressure in the reactor during a pulse can be made. Assuming that the pulse is uniformly distributed through the reactor, the average pressure over the duration of a pulse is on the order of 10 Torr.

Either one (single pulse) or two (double pulse) valves can be utilized in the TAP experiment. A pump–probe experiment is a special case of a double-pulse experiment in which reactants are introduced in an alternating sequence. In a typical pump–probe experiment the catalyst is first charged with a reactant pulse from the "pump" valve and later interrogated with a different pulse from the "probe" valve. The time (pump–probe interval) between the valve pulses can be varied between 0.001 and 0.500 s with an accuracy of 0.01 ms. Molecules in the pump pulse may form transient nondesorbing intermediates for which several reaction channels exist, even in the absence of the probe pulse. These adsorbed species can be reacted with the probe molecules to form gaseous products before they are transformed via competing reaction channels. Varying the time between the pump and probe pulses gives information related to the lifetime of surface intermediates. The product yield resulting from the reaction of the probe molecules with the adsorbed species reflects the amount of adsorbed species on the surface at the time of the probe pulse. The lifetime of the surface intermediate can be determined by measuring the product yield as a function of the pump–probe time interval.

The reactant pulses pass through the catalyst bed, and the products and unconverted reactants leaving the reactor pass through a series of collimating slits and are detected by a UTI 100C quadrupole mass spectrometer. Differential pumping between the reactor and the mass spectrometer removes molecules which are scattered by the collimating slits. The signal from the mass spectrometer is collected by an HP 3582A data acquisition unit coupled to an HP 9000 computer and the results of several pulses are averaged in order to improve the signal-to-noise ratio. Most of the data presented here were obtained by averaging the results from 100 pulses. In Fig. 2, a schematic of the input and product pulses from a TAP pump–probe experiment is depicted showing the relative pulse positions in a three-dimensional mass-time-intensity space. This figure illustrates the finite time delays for both C_2D_4 and O_2 following the pulse triggers as well as the formation of ethylene oxide and CO_2 on the silver catalyst.

In the experiments reported here the reactor was loaded with 0.5 g of silver powder (Aesar, 99.999%) sieved to give particles between 425 and 850 μm in diameter. The surface area was determined by krypton BET to be 0.08 $m^2\ g^{-1}$, giving a total surface area of the catalyst of approximately 400 cm^2. This surface area corresponds to approximately 4×10^{17} surface silver atoms. The silver powder was cleaned by pulsing O_2 through the reactor at 673 K until no CO_2 production could be detected. Note that 673 K is well above the recombination temperature of atomic oxygen on all three low-index planes of silver (*20–23*), as well as polycrystalline silver (*38, 39*), and also above the temperature for oxidation of surface carbon to CO_2 (*40, 41*). Thus, the surface should be free of both carbon and atomic oxygen following the oxidation treatment.

In all experiments reported here, the largest product peak ($m/q = 44$) was approximately 1% as intense as the reactant peaks, indicating that total conversion of reactants was on the order of 1%. This low conversion allows the TAP reactor to be treated as a differential reactor for data analysis. At low conversion mass spectrometric detection of product pulses is difficult for ions where interference from the reactant pulses is present. In the C_2D_4–O_2 reactant mixtures to form ethylene oxide and carbon dioxide, interference can occur at m/q ratios of 12, 14, 16, 24, 26, 28, 30, and 32. Interference at masses 15 and 29 also occurs due to the 1% natural abundance of ^{13}C. Consequently, detection and identification of products was done using m/q ratios of 40, 42, 44, 46, and 48. Production of water during the reaction was not monitored, but can be calculated from the amount of CO_2 formed and the stoichiometry of the total combustion reaction.

C_2D_4 (MSD Isotopes, 99%), O_2 (Matheson, Extra Dry), $^{18}O_2$ (Monsanto Research

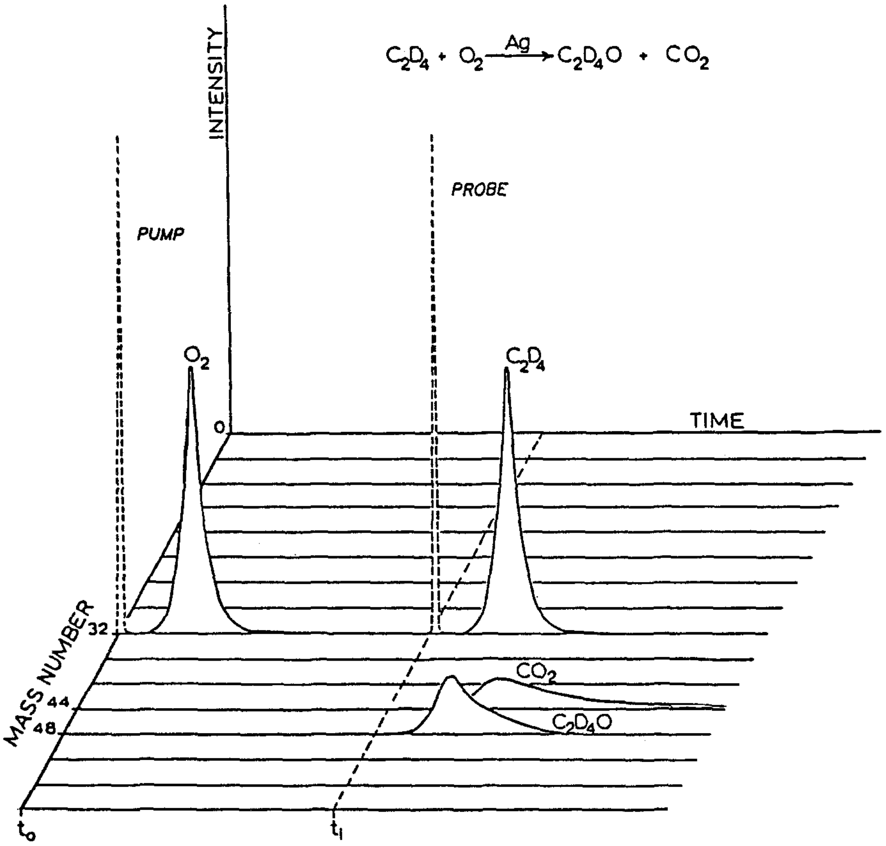

FIG. 2. Schematic of input and output data from a repetitive pump–probe experiment using O_2 pump and C_2D_4 probe molecules. The sharp dotted spikes correspond to the triggering of the pulse valves and the arrival of gas at the detector in the absence of a reactor.

Corp., 97% ^{18}O), CO_2 (Matheson, Bone Dry), and H_2 (Matheson, Prepurified) were all used as received.

RESULTS AND DISCUSSION

Reaction Dynamics

The product pulses resulting from a single pulse experiment with a 1 : 1 mixture of C_2D_4 and O_2 over the silver powder at 570 K are shown in Fig. 3. The largest product peak is observed at $m/q = 44$ and is assigned to CO_2 formation. Minor fragment peaks ($C_2D_2O^+$) of ethylene oxide or acetaldehyde overlap with the CO_2 peak but contribute at most 5% of the total area. The remaining product peaks occur at masses 42 (not shown), 46, and 48; these peaks have maximums at the same time, indicating that they arise from a common product. A comparison of the relative sizes of the peaks with published mass spectra of C_2H_4O and CH_3CHO (*24*) is shown in Table 1. The comparison in Table 1 relies on the assumption that fragmentation patterns of ethylene oxide and acetaldehyde do not change significantly upon deuterium substitution. This assumption is supported by published mass spectra of ethane (*29*) which show that fragmentation patterns differ by only 10–20% between C_2H_6 and C_2D_6. At this writing experimental mass spectra of deuterated ethylene oxide and acetaldehyde are not available. Inspection of Table 1 shows that the mass distribution measured here is in excellent agreement

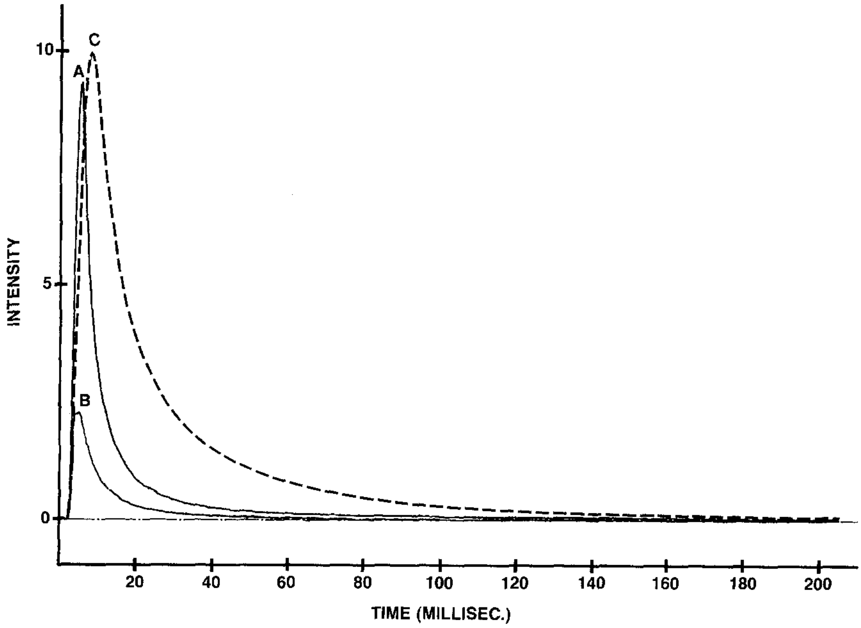

FIG. 3. Product peaks from oxidation of 1 : 1 mixture of C_2D_4 and O_2 at 570 K in a single-pulse experiment: (A) $m/q = 48$, $t_{max} = 4.4$ ms; (B) $m/q = 46$, $t_{max} = 4.4$ ms; (C) $m/q = 44$, $t_{max} = 6.6$ ms.

with the mass spectra of ethylene oxide but not with the acetaldehyde mass spectra. Thus, the product giving rise to the m/q = 42, 46, and 48 signals in Fig. 3 is identified as d_4-ethylene oxide. The possibility that a small amount of acetaldehyde also contributes to the m/q = 42, 46, and 48 peaks cannot be ruled out since the mass spectra of ethylene oxide and acetaldehyde are similar. However, the close agreement between the observed mass spectra and those published for ethylene oxide indicates that the selectivity to acetaldehyde is less than 10%. As a rule, the $m/q = 48$ signal was used to monitor d_4-ethylene oxide and the $m/q = 44$ signal was used to monitor CO_2.

The effect of temperature on ethylene oxide production is shown in Fig. 4. As expected, ethylene oxide production decreases monotonically with temperature. The value of t_{max} and the peak shape vary

TABLE 1

Comparison of Mass Spectrum of Reaction Product with Published Spectra for C_2H_4[a] and CH_3CHO[a]

		Relative magnitudes						
Fragment[a]	m/q[a]	Reaction product[a]	C_2H_4O (*24*)			CH_3CHO (*24*)		
$C_2H_4O^+(C_2D_4O^+)$	44(48)	(100)	100	100	100	100	100	100
$C_2H_3O^+(C_2D_3O^+)$	43(46)	(25)	25	23	22	58	57	56
$C_2HO^+(C_2DO^+)$	41(42)	(2.5)	<8	<4	<3	9	7	7

[a] Fragments and numbers in parentheses are for deuterated compounds.

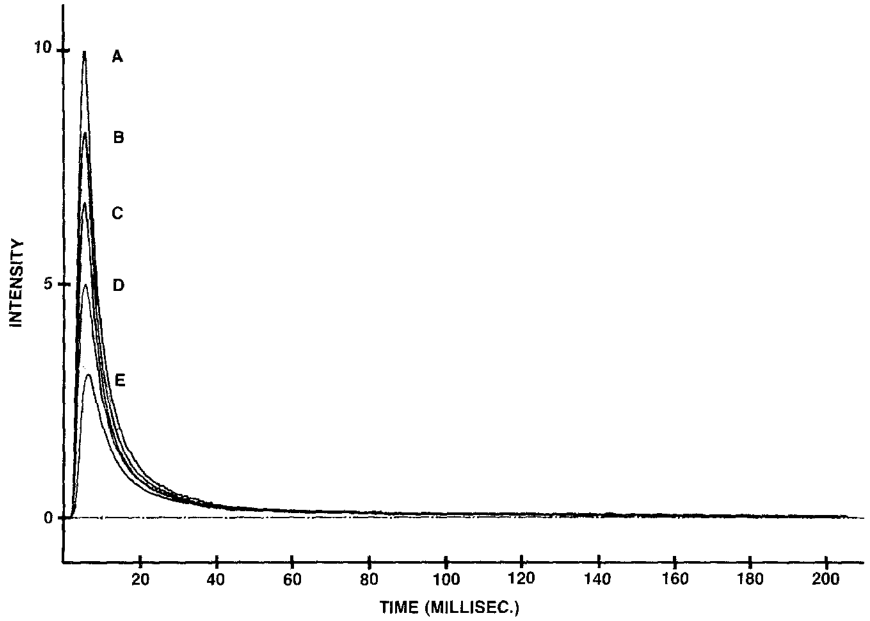

FIG. 4. Effect of temperature on C_2D_4O production from 1 : 1 mixture of C_2D_4 and O_2 in a single pulse. The temperatures and t_{max} values are: (A) 570 K, 4.6 ms; (B) 543 K, 4.6 ms; (C) 527 K, 4.8 ms; (D) 502 K, 5.4 ms; (E) 483 K, 5.8 ms. For reference, argon exhibits a t_{max} of 3.5 ms at 570 K.

only slightly with temperature. These small variations can be entirely accounted for by changes in the time of flight between the reactor and the mass spectrometer as the temperature changes, indicating that ethylene oxide adsorbs very weakly on the silver surface (*19*). If strong adsorption were occurring, the average surface lifetime of the ethylene oxide would exhibit a strong variation with temperature, resulting in large changes of t_{max}. Weak adsorption of ethylene oxide on the silver powder is consistent with studies of ethylene oxide adsorption on Ag(110) (*26, 27*), where the heat of adsorption has been found to be ~10 kcal/mol. Since the TAP reactor operates in a differential mode, the areas under the curves in Fig. 4 are a measure of the relative rates of ethylene oxide formation. These rates were used to construct the Arrhenius plot of Fig. 5. The activation energy (E_a) for ethylene oxide formation is approximately 4.5 kcal/mol over the temperature range investigated. Similar values of E_a have been reported previously at temperatures near 580 K (*13, 15, 28*). This activation energy can be interpreted most simply as the difference between the activation energies for reaction of adsorbed oxygen and ethylene and ethylene desorption. Given this interpretation, the activation energy for the surface reaction is approximately 15 kcal/mol. At 450 K the activation energy reported in the previous work increased substantially.

The effect of temperature on CO_2 production is shown in Fig. 6. In contrast to ethylene oxide, the CO_2 product shows a striking variation in peak shape and t_{max} with temperature. The CO_2 pulses are also considerably broader, indicating that CO_2 is strongly adsorbed by the silver surface. This possibility was tested by pulsing CO_2 over an oxidized catalyst at reaction temperature and comparing its pulse shape with the CO_2 formed in an ethylene reaction run under analogous conditions. The two CO_2 pulses are plotted in Fig. 7. The close similarity of the two pulses confirms that the shape of the CO_2 product pulse is

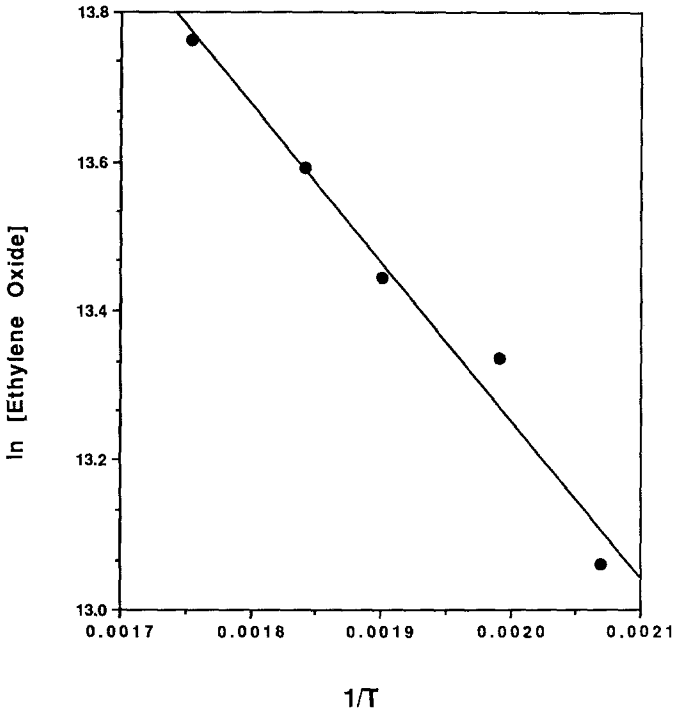

FIG. 5. Arrhenius plot for C_2D_4O production from 1 : 1 mixture of C_2D_4 and O_2. The relative rate was obtained from the area under the *m*/*q* curves of Fig. 4.

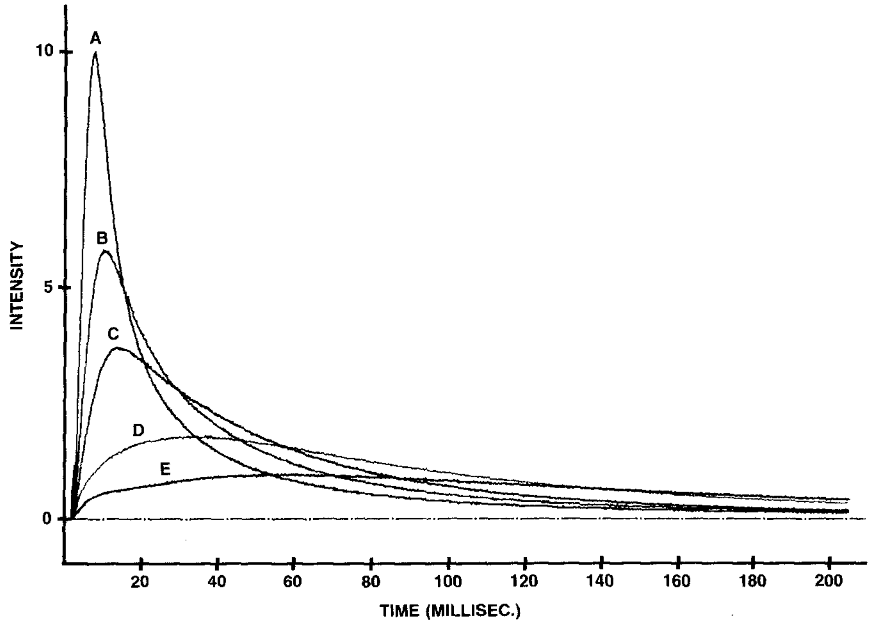

FIG. 6. Effect of temperature on CO_2 production from 1 : 1 mixture of C_2D_4 and O_2 in a single pulse. The temperatures and t_{max} values are: (A) 570 K, 6.6 ms; (B) 543 K, 9.6 ms; (C) 527 K, 13.2 ms; (D) 502 K, 36.6 ms; (E) 483 K, 72 ms.

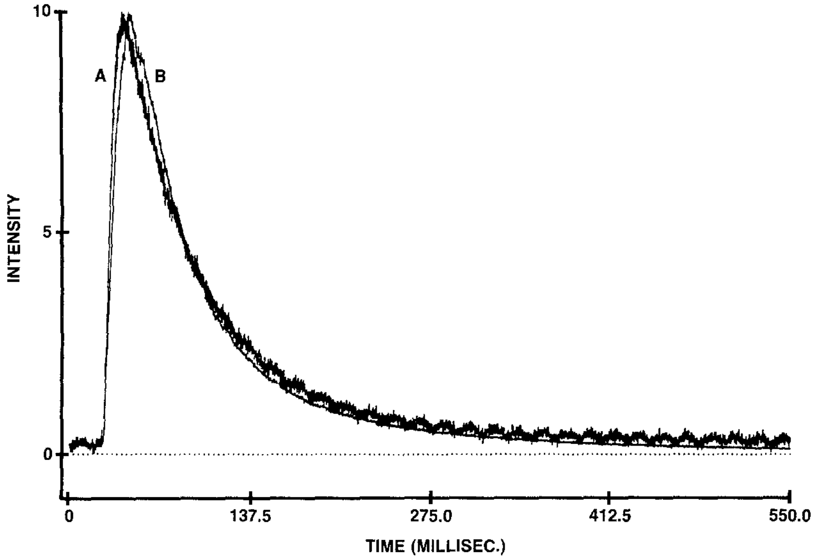

FIG. 7. Comparison at 523 K of (A) CO_2 adsorption curve from pulsing CO_2 over an oxygen-covered surface and (B) CO_2 product curve from reaction of O_2 and C_2D_4 in the single-pulse experiment of Fig. 6.

determined by CO_2 adsorption/desorption and not by the kinetics of the surface reaction between ethylene and oxygen. The CO_2 adsorption most probably involves a reaction with $O_{(a)}$ to form an adsorbed carbonate species. On silver single-crystal surfaces carbonate is stable below 480 K and decomposes with an activation energy of 27.5 kcal/mol (*21*, *23*). The slight differences in the two curves may be due to coverage-dependent kinetics for carbonate decomposition.

Under steady-state conditions at high pressure the selectivity of ethylene oxidation to form ethylene oxide is known to be directly proportional to the oxygen concentration (*2*). The dependence of the relative product yield on reactant ratio was examined qualitatively in TAP pump–probe experiments. The experiments were performed by pulsing different amounts of oxygen and ethylene into the microreactor and monitoring the CO_2 and ethylene oxide yield as a function of the O_2/C_2D_4 ratio. The experiment was arranged so that the ethylene valve was fired 210 ms after the oxygen valve. At this delay time the concentration of gas-phase oxygen is at least two orders of magnitude below its maximum during the oxygen pulse.

Product curves for a series of pump–probe experiments are plotted in Fig. 8. In both data sets the oxygen pulse occurs at $t = 0$. Ethylene oxide production was observed after the injection of ethylene but not after the injection of oxygen, while CO_2 production occurred at both times. The relative yields of both products are represented in Fig. 9 for varying reactant ratios. From measurements of this type we determined that the amount of both ethylene oxide and CO_2 formed increases nearly linearly with the size of the oxygen pulse for $O_2 : C_2D_4$ ratios below 0.6 and becomes nearly independent of the O_2 pulse size for high $O_2 : C_2D_4$ ratios. Depending on reaction conditions, values between 0 and 1 have been reported previously for the reaction orders of oxygen and ethylene (*1*, *2*, *15*).

Results of the pump–probe experiments demonstrate that the rate of ethylene oxidation depends on the concentration of adsorbed oxygen and that at sufficiently high

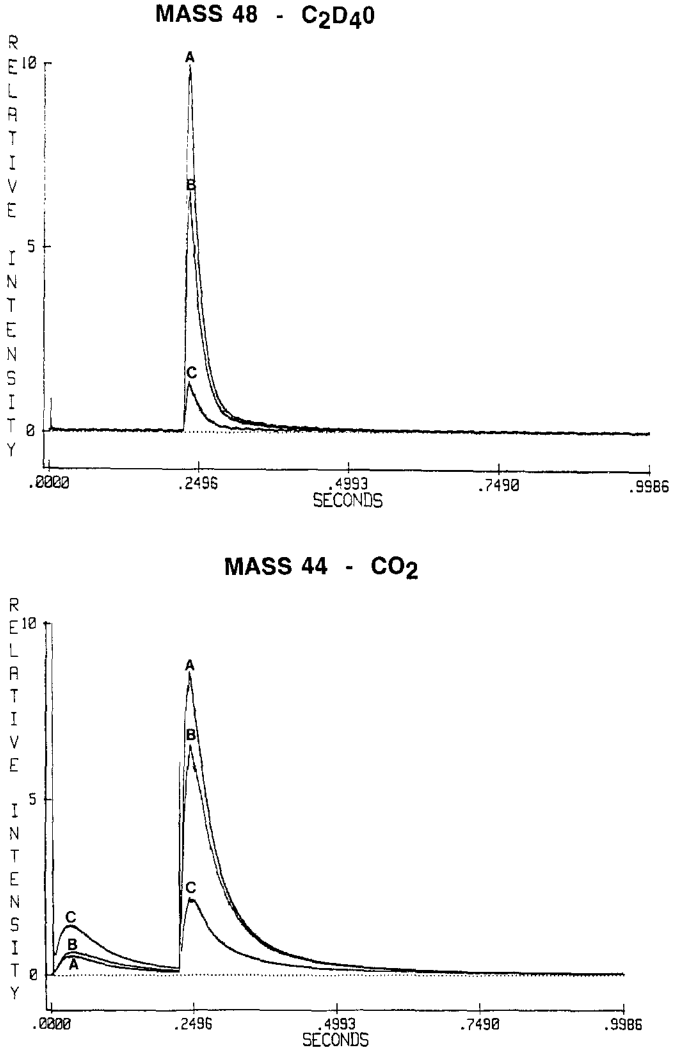

FIG. 8. Series of product curves using O_2 pump and C_2D_4 probe molecules with the relative area ratios of reactants transmitted through the reactor [O_2 to C_2D_4] of (A) 5; (B) 1; and (C) 0.5. Injection times are at 0 s for O_2 and 0.210 s for C_2D_4 at 523 K catalyst temperature.

oxygen pulse intensities the rate becomes independent of the oxygen coverage. They also indicate that selective oxidation to ethylene oxide involves the reaction of ethylene with adsorbed oxygen species with no measurable reaction time, as both ethylene and ethylene oxide appear simultaneously at the reactor exit.

Mechanism

One of the main questions about the mechanism of ethylene oxidation is the role(s) of adsorbed molecular and atomic oxygen. Knowledge of the average surface lifetime of the active oxygen species allows the identification of the form of the adsorbed active oxygen. Molecular oxygen is very weakly bound to silver surfaces (*21, 22, 31, 32*), desorbing below 200 K under vacuum. Atomic oxygen, on the other hand, is stable at temperatures up to about 600 K, undergoing associative desorption above this temperature on all three low-index faces of silver (*21–23, 31*), as well as

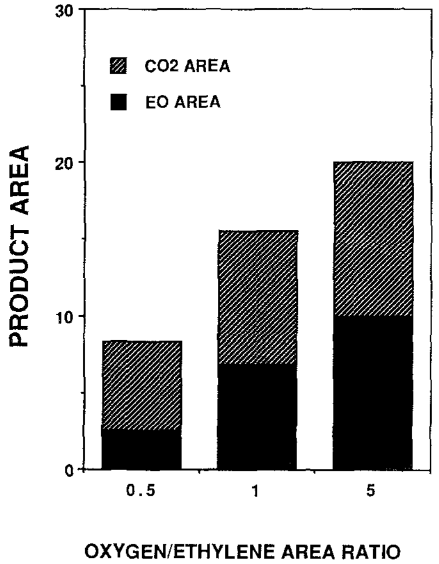

FIG. 9. Relative amounts of CO_2 and C_2D_4O formed in ethylene oxidation versus the reactant ratios in the O_2 pump and the C_2D_4 probe pulses at 523 K catalyst temperature.

on polycrystalline silver (*38, 39*). Thus, molecular oxygen should have a very short surface lifetime at the temperatures for catalytic ethylene oxidation, while atomic oxygen should have a relatively long lifetime. Table 2 lists expected surface half-lives of molecular and atomic oxygen estimated from desorption kinetics measured on Ag(110) (*23, 42*). The surface lifetime of molecular oxygen is five orders of magnitude less than atomic oxygen at 525 K.

TAP pump–probe experiments provide a direct measure of the lifetime of the adsorbed oxygen intermediate. As described earlier, these experiments are performed by alternately pulsing reactants from two high-speed valves and varying the pump–probe interval. To measure the lifetime of the active oxygen species the pulse intensities of oxygen and ethylene were held constant, and the delay interval was changed. The surface lifetime of active oxygen species was investigated by measuring the C_2D_4O product yield as a function of the pump–probe interval.

Figure 10 shows the C_2D_4O yield from a series of pump–probe experiments carried out at 523 K. The oxygen pump pulse was introduced at $t = 0$ and the ethylene probe pulses followed at varying intervals. Remarkably, the maximum C_2D_4O yield did not occur when both gas phase reactants were at a maximum concentration, i.e., narrowly separated in time. Instead, it was observed at a pump–probe interval of 120 ms, when the gas-phase oxygen concentration was close to zero. This result clearly shows that the maximum concentration of active adsorbed oxygen is formed well after the injection of the oxygen pulse.

The delayed maximum may be due to surface carbonate formation and decomposition. During the oxygen pulse some CO_2 is formed due to the oxidation of surface carbon deposited during the previ-

TABLE 2

Surface Half-Lives for Adsorbed Atomic and Molecular Oxygen on Ag(110)

	Half-life(s)		
Temperature (K)	Atomic oxygen[a]	Molecular oxygen[b]	Molecular oxygen[c]
475	3600	5.8×10^{-4}	8×10^{-9}
500	410	4.6×10^{-4}	4×10^{-9}
525	58	3.9×10^{-4}	2.7×10^{-9}
550	10	3.2×10^{-4}	1.6×10^{-9}
575	2	2×10^{-4}	1.1×10^{-9}

[a] Based on the rate constant $k = (2 \times 10^{15}\ s^{-1}) \exp(-20808/T)$ (*23*).
[b] Based on the rate constant $k = (1.6 \times 10^{5}\ s^{-1}) \exp(-2345/T)$ (*42*).
[c] Based on the rate constant $k = (10^{13}\ s^{-1}) \exp(-5533/T)$ (*42*).

ous ethylene pulse. If the CO_2 then reacts with $O_{(a)}$ to form carbonate, it decreases the available $O_{(a)}$ and inhibits ethylene oxidation. As the carbonate decomposes and CO_2 exits the reactor, the concentration of $O_{(a)}$ increases and the surface becomes more active. The resulting effect would be suppression of C_2D_4O production at short pump–probe intervals when the concentration of surface carbonate is highest. In support of this explanation is the fact that the maximum in C_2D_4O production occurs when roughly 90% of the CO_2 formed during the oxygen pulse has left the reactor.

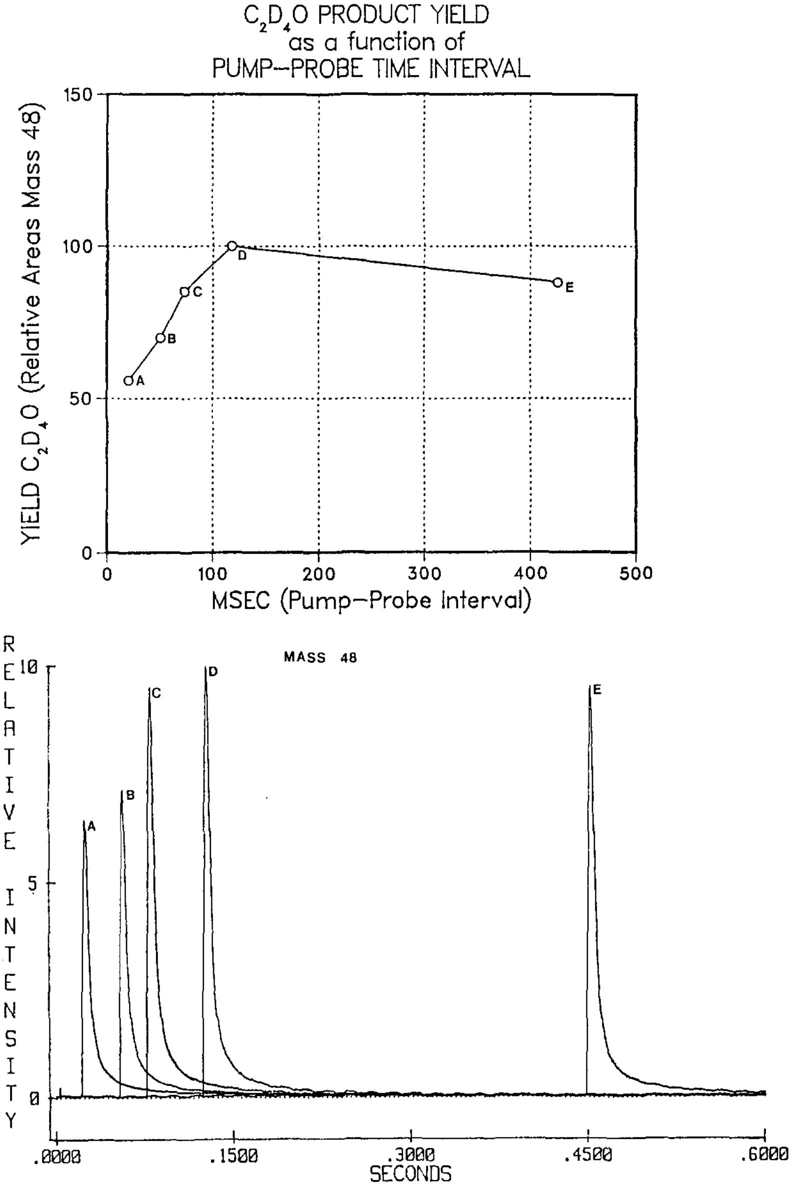

FIG. 10. Series of C_2D_4O product areas and product curves using O_2 pump and C_2D_4 probe molecules at 523 K catalyst temperature with the following intervals between the O_2 pump and C_2D_4O probe: (A) 20 ms; (B) 50 ms; (C) 72 ms; (D) 117 ms; (E) 425 ms.

Additional support for this explanation comes from the observation that at very high oxygen to ethylene ratios, when the amount of deposited carbon is lower, the effect is less pronounced.

An alternate explanation for the increases in C_2D_4O production involves the rearrangement of surface or subsurface oxygen atoms. Backx *et al.* (*10*) and Haul and Neubauer (*18*) have obtained evidence suggesting that the presence of subsurface oxygen, formed by diffusion of surface oxygen atoms into the subsurface region (*31*), is necessary for epoxidation to occur. In the absence of subsurface oxygen, only total combustion occurs (*10*). Immediately upon introduction of the oxygen pulse, the concentration of subsurface oxygen may be fairly low. Introducing a delay before the C_2D_4 pulse may allow sufficient time for diffusion of oxygen into subsurface states, thereby resulting in the observed increase in C_2D_4O production. Unfortunately, the possible inhibition of this reaction by CO_3 precludes isolation of this effect.

The slow decrease of C_2D_4O and CO_2 production with delay times greater than 120 ms is due to slow desorption of the active oxygen species for ethylene oxidation. The data of Fig. 10 clearly show that the oxygen species involved in ethylene oxidation are stable on the surface for times at least on the order of seconds at 547 K. Additional information regarding the surface lifetime of the active oxygen was obtained by exposing the silver powder to 200 O_2 pulses at 547 K, and then pulsing pure C_2D_4 repeatedly at fixed intervals over the catalyst, also at 547 K. The change in the amount of product formed as a function of the number of C_2D_4 pulses is shown in Fig. 11. Product formation can still be observed after 10 ethylene pulses and a total elapsed time of 3000 ms. By repeating the experiment shown in Fig. 10 at 523 K, it was found that waiting 300 s between the final O_2 pulse and the initial ethylene pulse resulted in a 50% decrease in the amount of product formed by the initial pulse. Thus, at 523 K, the active oxygen species has a half-life of approximately 5 min.

The results shown in Figs. 10 and 11 provide strong evidence that, under the conditions used here, atomic oxygen is the active species for both epoxidation and total combustion. The surface lifetime of the active species is much greater than that expected for molecular oxygen on either clean (*21, 22, 31, 32*) or alkali metal-doped (*33, 34*) silver single-crystal surfaces (see Table 2). Atomic oxygen, on the other hand, is much more stable than molecular oxygen (*20–23, 31*). On the basis of the desorption kinetics measured by Bowker *et al.* (*23*) on Ag(110), atomic oxygen would be expected to have a half-life of approximately 10 s at 547 K and 100 s at 523 K over a range of coverage between 0.05 and 0.50 monolayer. These numbers are in excellent order of magnitude agreement with the half-life of the active oxygen measured here, providing strong support for a mechanism involving atomic oxygen in both the epoxidation and combustion reaction.

In contrast to the active oxygen species, ethylene has a very short surface lifetime. In experiments where an ethylene pulse was followed by a delayed oxygen pulse, no ethylene oxide formation was ever observed simultaneously with the oxygen pulse, even for delay times as short as 10 ms. Thus, the active ethylene species is very weakly adsorbed, as expected from studies of ethylene adsorption on single-crystal surfaces (*27, 35*). Some CO_2 production was observed during the O_2 pulse, presumably due to oxidation of surface carbon (*40, 41*) deposited during the ethylene pulse. The results of the pump–probe experiments reported here are in qualitative agreement with the earlier work of Mikami *et al.* (*36*).

It is conceivable that the introduction of ethylene into the reactor could induce desorption of some O_2 and that this species reacts to form ethylene oxide. If so, this reaction must be very efficient as no dioxygen is observed to exit the reactor when

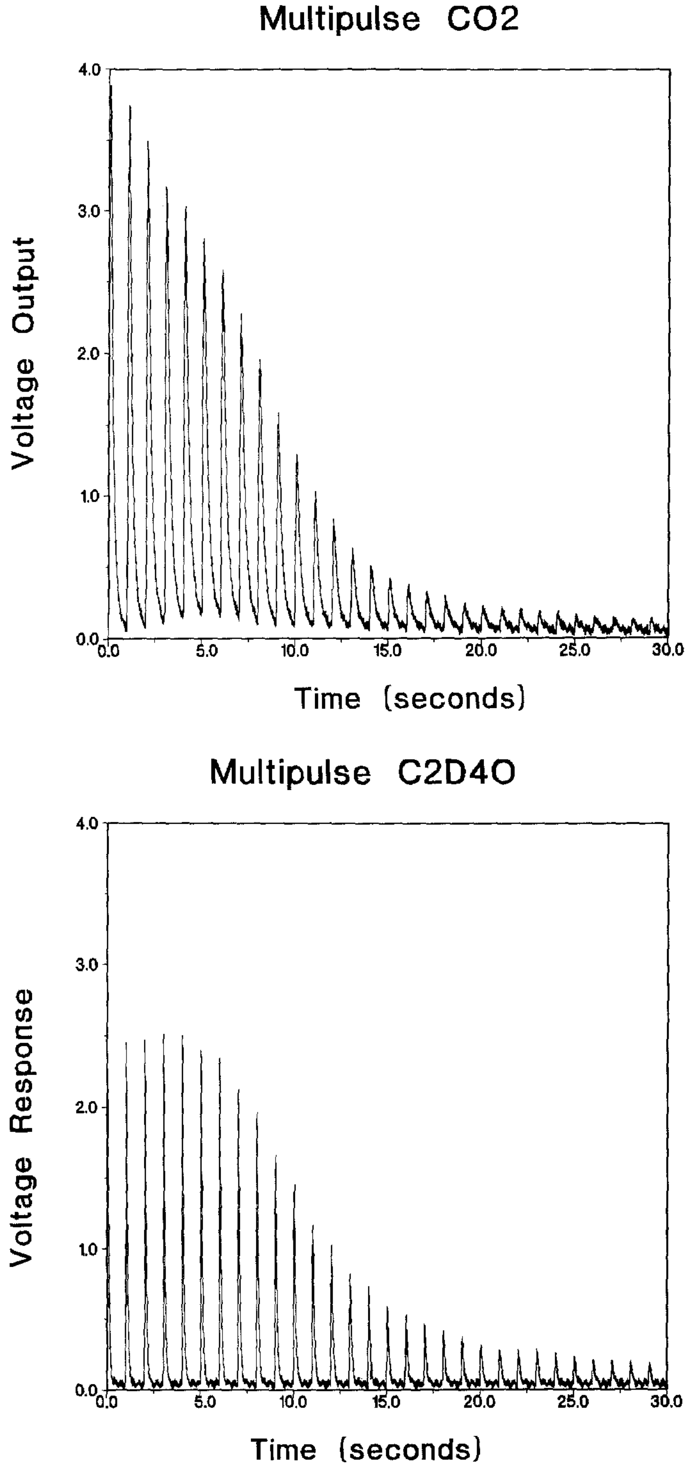

FIG. 11. Amounts of product (A) CO_2 and (B) C_2D_4O formed as a function of the time with repeated pulses of anaerobic C_2D_4 at 547 K. The catalyst was pretreated with 200 O_2 pulses at 547 K.

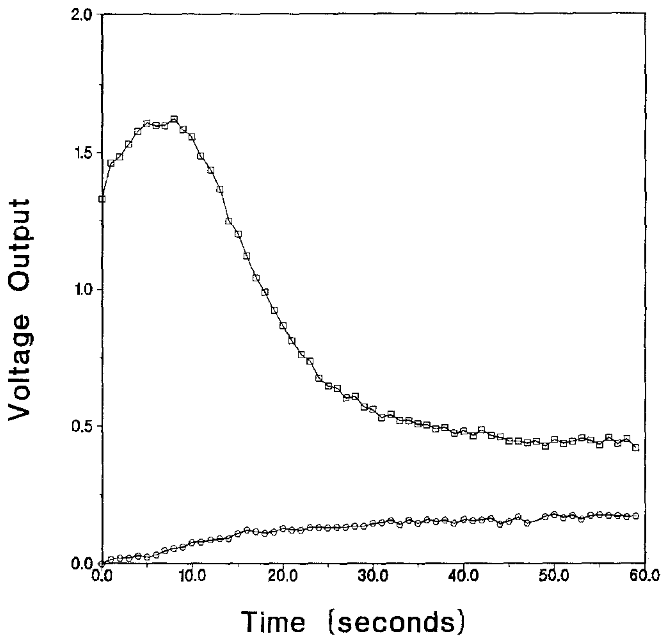

FIG. 12. Multipulse data plotting the peak maximum of products $C_2D_4{}^{16}O$ (squares) and $C_2D_4{}^{18}O$ (circles) as a function of pulse number when C_2D_4 and $^{18}O_2$ were pulsed from separate valves over a silver catalyst preoxidized with ^{16}O. The reactor temperature was 493 K. In the data shown the $^{18}O_2$ pulse leads the C_2D_4 pulse by 10 ms.

perhydridoethylene is pulsed in pump–probe experiments, whereas ethylene oxide is abundantly produced. Further, if O_2 were the reactive species, we would expect the maximum yield of ethylene oxide to correspond to the highest concentration of O_2 in the reactor in the experiments shown in Figs. 10 and 11, namely, at zero time delay when the gas-phase dioxygen is still in the reactor. The data are in conflict with this interpretation, but, as discussed above, possible inhibition by carbon dioxide complicates this matter. In order to test the possible involvement of dioxygen further we pulsed C_2D_4 and $^{18}O_2$ over a surface presaturated with ^{16}O, and the product signal was monitored as the train of C_2D_4 and $^{18}O_2$ pulses were injected into the reactor. The interval between the oxygen and ethylene pulses was initially adjusted to 10 ms, since at this time approximately half of the dioxygen pulse is discharged from the reactor. Identical results were obtained for delay times of 5 and 1.0 ms. The signal was collected at a delay time corresponding to a maximum in the product signal. The points shown in Fig. 12 for the two oxygen isotopes of ethylene oxide were each signal-averaged for 60 ethylene pulses at a pulse rate of 1 s^{-1}. No $C_2D_4{}^{18}O$ was observed during the first set of 60 pulses! The results show that the O_2 present in the gas phase is not incorporated into the product over the preoxidized catalyst. Furthermore, it is clear that the reactivity of the predosed surface oxygen is at least an order of magnitude greater than that due to the $^{18}O_2$ even after 10 s. The slow increase in the yield of the heavier species is consistent with a mechanism involving dissociation of $^{18}O_2$ on a partially reduced surface and the exchange of surface and subsurface oxygen.

The role of subsurface oxygen in ethylene oxidation on silver is not well understood. Subsurface oxygen is formed upon exposure of silver to O_2 above 420 K and does not desorb at temperatures up to 720 K (*31*). Subsurface oxygen does, however, undergo exchange with surface atomic oxygen, as evidenced by isotopic labeling experiments (*31*). Backx *et al.* (*10*) and Haul and Neubauer (*18*) have claimed that subsurface oxygen is necessary for epoxidation to occur. This result could not be confirmed in the TAP experiments reported here since, at temperatures low enough to avoid formation of subsurface oxygen, the sensitivity of the detection system was too low to observe any product formation. It was possible to demonstrate, however, that subsurface oxygen becomes incorporated into the reaction products. Subsurface states were populated with ^{18}O by exposing the catalyst to 1000 pulses of $^{18}O_2$ at 570 K. This temperature is near the associative desorption peak temperature of $O_{(a)}$ on Ag(110) (*23*), Ag(111) (*22*), and polycrystalline silver (*38, 39*). Thus surface $^{16}O_{(a)}$ should rapidly recombine and desorb at 570 K, leaving only subsurface ^{18}O. Following population of subsurface states with ^{18}O, a 1 : 1 mixture of C_2D_4 and O_2 was pulsed over the catalyst at 570 K and the mass 50 signal was monitored to detect incorporation of ^{18}O into the ethylene oxide. The results of this experiment are shown in Fig. 13. Curve A represents an average of the first 10 pulses and is approximately $\frac{1}{8}$ as large as the C_2D_4O peak at $m/q = 48$. Thus, a substantial fraction of the ethylene oxide formed during ethylene oxidation incorporates subsurface oxygen. This incorporation presumably occurs via exchange of subsurface $^{18}O_{(a)}$ with surface $^{16}O_{(a)}$, followed by reaction of the resulting surface $^{18}O_{(a)}$ with ethylene. As the total number of pulses was increased, the amount of ^{18}O incorporated into the products gradually decreased. Even after more than 100 pulses, however, some $m/q = 50$ signal could still be detected. By repeating the experiment described above, and monitoring the $m/q = 46$ signal instead of the $m/q = 50$ signal, it was found that subsurface

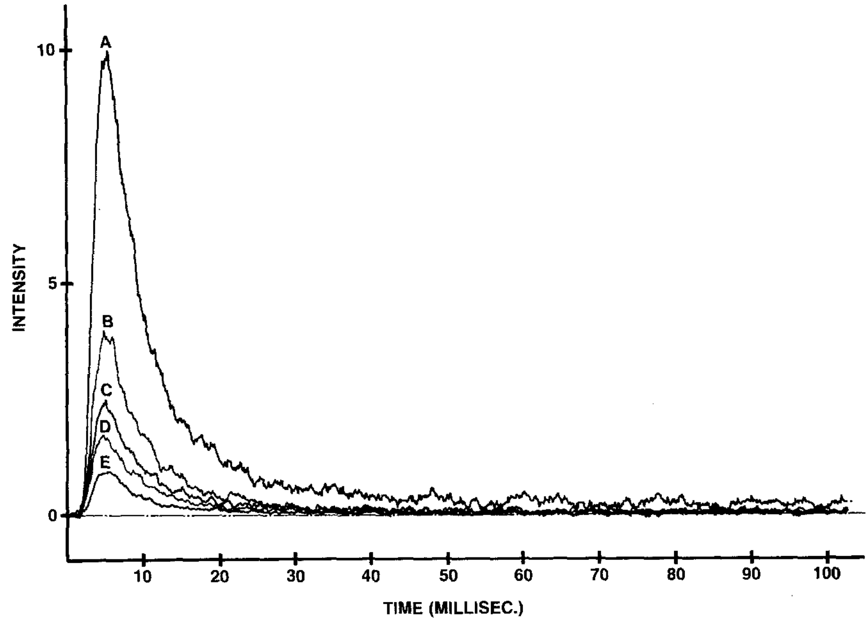

FIG. 13. Incorporation of subsurface oxygen into ethylene oxide. After populating the subsurface states with ^{18}O, a 1 : 1 mixture of C_2D_4 and O_2 was pulsed over the catalyst. The $m/q = 50$ (corresponding to $C_2D_4{}^{18}O$) product curve is plotted in the following subgroups: (A) average of pulses 1 through 10; (B) average of pulses 11 through 30; (C) average of pulses 31 through 50; (D) average of pulses 51 through 90; (E) average of pulses 91 through 170.

oxygen is incorporated into the carbon dioxide as well as the ethylene oxide.

Several workers have reported the observation of acetic acid or acetate as an intermediate in the total combustion of ethylene (*12, 37*). Because of the very short contact times obtained in the TAP experiment, desorbing reaction intermediates which undergo further reaction in more conventional reactors can often be detected by TAP (*19*). Under the reaction conditions used here, however, no signal was ever observed at $m/q = 60$, the parent peak of acetic acid. Nor was any acetic acid observed if the reaction was stopped and hydrogen pulsed over the catalyst. This finding is in contrast to the work of Kobayashi and Kanno (*37*), who observed acetic acid formation when hydrogen was flowed over their catalyst following reaction. Our results do not preclude the possibility that acetic acid or acetate are formed under reaction conditions different from those used here.

CONCLUSION

The results of this study have provided several important insights into the type of adsorbed oxygen participating in ethylene oxidation. First, it is clear that adsorbed molecular oxygen, whether formed by adsorption from the gas phase or recombination of $O_{(a)}$, is not involved in the formation of ethylene oxide in the experiments reported here. Second, the rate of ethylene oxidation depends on the concentration of $O_{(a)}$, and the selective oxidation involves a reaction of ethylene with this species with a time constant dictated primarily by the rate constants for ethylene and ethylene oxide desorption. The rate constant for oxygen addition is not distinguishable from these fast processes. Third, TAP experiments using ^{18}O show that subsurface oxygen is incorporated into both CO_2 and ethylene oxide during ethylene oxidation. Fourth, pump–probe experiments indicate that CO_2 is strongly adsorbed at reaction temperatures and may affect catalytic activity by reacting with $O_{(a)}$ to form surface carbonate.

The results of this study are also relevant to a more general question related to the connection between applied and fundamental catalyst research. Most applied research programs work with bulk catalyst samples and employ conventional reactor systems, operating close to plant conditions. Serious complications in understanding mechanisms may be introduced by secondary reactions or transport effects. In contrast, fundamental studies using sophisticated surface science techniques are usually conducted with model catalysts such as well-defined single crystals. The TAP experiment may help span the gap between these two experimental regimes and indicate the correspondence between them.

ACKNOWLEDGMENTS

One of us (R.J.M.) gratefully acknowledges the support of the National Science Foundation (NSF CBT 87-01342) throughout the course of this work. The cooperation of Monsanto in facilitating this joint research is also gratefully acknowledged.

REFERENCES

1. Sachtler, W. M. H., Backx, C., and van Santen, R. A., *Cat. Rev. Sci. Eng.* **23,** 127 (1981).

2. Verykios, X. E., Stein, F. P., and Coughlin, R. W., *Cat. Rev. Sci. Eng.* **22,** 197 (1980).

3. Voge, H. H., and Adams, C. R., *in* "Advances in Catalysis" (D. D. Eley, H. Pines, and P. B. Weisz, Eds.), Vol. 17, p. 51. Academic Press, New York, 1967.

4. Kilty, R. A. and Sachtler, W. M. H., *Cat. Rev. Sci. Eng.* **10,** 1 (1974).

5. Stoukides, M., and Vayenas, C. G., *J. Catal.* **69,** 18 (1981).

6. Stoukides, M., and Vayenas, C. G., *J. Catal.* **70,** 137 (1981).

7. Akimoto, M., Ichikawa, K., and Echigoya, E., *J. Catal.* **76,** 333 (1982).

8. Force, E. L., and Bell, A. T., *J. Catal.* **40,** 356 (1975).

9. Force, E. L., and Bell, A. T., *J. Catal.* **38,** 440 (1975).

10. Backx, C., Moolhuysen, J., Greenen, P., and van Santen, R. A., *J. Catal.* **72,** 364 (1981).

11. van Santen, R. A., and de Groot, C. P. M., *J. Catal.* **98,** 530 (1986).

12. Grant, R. B., and Lambert, R. M., *J. Catal.* **92,** 364 (1985).

13. Campbell, C. T., and Paffett, M. T., *Surf. Sci.* **139,** 396 (1984).
14. Campbell, C. T., and Paffett, M. T., *Appl. Surf. Sci.* **19,** 28 (1984).
15. Campbell, C. T., *J. Catal.* **94,** 436 (1985).
16. Campbell, C. T., and Koel, B. E., *J. Catal.* **92,** 272 (1985).
17. Campbell, C. T., *J. Catal.* **99,** 28 (1986).
18. Haul, R., and Neubauer, G., *J. Catal.* **105,** 39 (1987).
19. Gleaves, J. T., Ebner, J. R., and Kuechler, T. C., *Cat. Rev. Sci. Eng.* **30,** 49 (1988).
20. Engelhardt, H. A., and Menzel, D., *Surf. Sci.* **57,** 591 (1976).
21. Campbell, C. T., and Paffett, M. T., *Surf. Sci.* **143,** 517 (1984).
22. Campbell, C. T., *Surf. Sci.* **157,** 43 (1985).
23. Bowker, M., Barteau, M. A., and Madix, R. J., *Surf. Sci.* **92,** 528 (1980).
24. "Eight Peak Index of Mass Spectra," 3rd. ed., Vol. I. Royal Society of Chemistry, Nottingham, UK, 1983.
25. van Santen, R. A., and Kuipers, H. P. C. E., *in* "Advances in Catalysis" (D. D. Eley, H. Pines, and P. B. Weisz, Eds.), Vol. 35, p. 65. Academic Press, New York, 1987.
26. Campbell, C. T. and Paffett, M. T., *Surf. Sci.* **177,** 417 (1986).
27. Backx, C., de Groot, C. P. M., Biloen, P., and Sachtler, W. M. H., *Surf. Sci.* **128,** 81 (1983).
28. Dettwiler, H. R., Baiker, A., and Richarz, W., *Helv. Chim. Acta* **62,** 1689 (1979).
29. Amenomiga, Y., and Potlie, R. F., *Canad. J. Chem.* **46,** 1735 (1968).
30. Haul, R., Hoge, D., Neubauer, G., and Zeek, U., *Surf. Sci.* **122,** 6622 (1982).
31. Backx, C., de Groot, C. P. M., and Biloen, P., *Surf. Sci.* **104,** 300 (1981).
32. Barteau, M. A., and Madix, R. J., *Surf. Sci.* **97,** 101 (1980).
33. Kitson, M., and Lambert, R. M., *Surf. Sci.* **109,** 60 (1981).
34. Spencer, N. D., and Lambert, R. M., *Chem. Phys. Lett.* **83,** 388 (1981).
35. Barteau, M. A., and Madix, R. J., *Surf. Sci.* **103,** L171 (1981).
36. Mikami, J., Shatoh, Sh., and Kobayashi, H., *J. Catal.* **18,** 265 (1970).
37. Kobayashi, M., and Kanno, T., *J. Catal.* **90,** 24 (1984).
38. Ekern, R. J., and Czanderna, A. W., *J. Catal.* **46,** 109 (1977).
39. Kagawa, S., Iwamoto, M., and Morita, S., *J. Chem. Soc. Faraday Trans. 1* **78,** 143 (1982).
40. Barteau, M. A., and Madix, R. J., *J. Amer. Chem. Soc.* **105,** 344 (1983).
41. Barteau, M. A., and Madix, R. J., *Surf. Sci.* **115,** 355 (1982).
42. Barteau, M. A., and Madix, R. J., *Surf. Sci.* **97,** 101 (1980).